Neurosurgical Review (2026) 49:24
https://doi.org/10.1007/s10143-025-03901-7

REVIEW

# Can artificial intelligence accurately predict the risk of hematoma expansion in intracerebral hemorrhage? A systematic review and Meta-analysis of 7,665 patients

**Ibrahim Mohammadzadeh[1] · Bardia Hajikarimloo[2] · Shahin Mohammadzadeh[1] · Amin Mohamad Niaei[3] · Paniz Sanjari Pirayvatloo[4] · Mohammad Amin Habibi[5] · Poriya Minaee[1] · Adam A. Dmytriw[6] · Ahmet Günkan[7] · Pascal Jabbour[8]**

Received: 29 July 2025 / Revised: 30 September 2025 / Accepted: 19 October 2025


## Abstract

Early prediction of hematoma expansion (HE) in patients with intracerebral hemorrhage (ICH) is critical for improving clinical outcome and guiding timely interventions. This study focuses on assessing the effectiveness of artificial intelligence (AI) models, specifically those utilizing machine learning (ML) and deep learning (DL) in predicting HE. The search strategy for this study was conducted in PubMed, Scopus, Embase, and Web of Science to identify eligible studies. Metrics such as sensitivity, specificity and area under the curve (AUC) were extracted and analyzed. Out of 1,235 studies initially screened, 14 met the inclusion criteria with totally 7665 patients. AI algorithms demonstrated significant predictive capabilities. The pooled sensitivity and specificity across studies were 0.82 [95% CI: 0.74–0.88] and 0.83 [95% CI: 0.78–0.87], respectively. The pooled positive DLR was 4.91 [95% CI: 3.73–6.47], while the negative DLR was 0.21 [95% CI: 0.14–0.32]. The diagnostic score was 3.14 [95% CI: 2.55–3.72], and the overall diagnostic odds ratio was 23.01 [95% CI: 12.83–41.24]. The pooled AUC was 0.89, suggesting a potentially useful diagnostic performance, although the high heterogeneity limits the robustness of this finding. Subgroup analysis revealed that AI models performed better in predicting HE, in patients with spontaneous ICH compared to patients with traumatic brain injury-related ICH, with a higher AUC (0.90 vs. 0.87), sensitivity (0.85 vs. 0.76) and diagnostic odds ratio (28 vs. 16). AI-based models may serve as potentially useful tools in predicting HE and supporting clinical decisions in ICH care. However, due to the high heterogeneity across studies, these findings should be interpreted with caution, and rigorous external validation with standardized imaging protocols is essential before clinical implementation.

**Keywords** Intracerebral hemorrhage · Hematoma expansion · Artificial intelligence · Machine learning · Deep learning · Diagnostic performance

## Introduction

Intracerebral hemorrhage (ICH) is a life-threatening neurological condition associated with high morbidity and mortality rates, accounting for about 20% of all strokes worldwide [1, 2]. One of the significant complications of this disease is hematoma expansion, which typically occurs within the first 24 to 48 h after onset and represents one of the critical clinical challenges in the treatment and management of spontaneous and traumatic ICH [3, 4]. Traumatic hematomas usually result from external forces causing a traumatic brain injury with intracranial hemorrhage [5, 6]. In contrast, spontaneous hemorrhages can have multiple non-traumatic causes, such as hypertension or vascular abnormalities [3, 7]. In both categories, the gradual enlargement of the hematoma can cause an elevation of the intracranial pressure associated with serious neurologic deficits, poor prognosis, and high rates of disability and mortality [3, 8, 9].

Artificial intelligence models, especially machine learning (ML) and deep learning (DL) have been widely used in many fields of medicine, including diagnosing and treating

Ibrahim Mohammadzadeh and Bardia Hajikarimloo contributed equally to this work.

Extended author information available on the last page of the article

Published online: 24 November 2025

cerebrovascular disease [10–14]. Studies demonstrated that AI models have higher sensitivity and specificity in predicting early hematoma expansion [15]. AI has different algorithms to predict hematoma expansion. These algorithms are based on features such as baseline hematoma volume, imaging biomarkers, and clinical variables to predict the expansion of hematoma [16]. Several studies have investigated the value of AI for diagnosis [17], radiographic evaluation and management of ischemic and hemorrhagic strokes, arteriovenous malformations, and aneurysms [10]. Although AI has shown significant improvements in the predictability of hematoma expansion, variability in imaging protocols and feature extraction techniques has raised concerns about the validity of those studies.

Therefore, this study evaluates the application of AI models in predicting HE risks among patients with ICH. By systematically assessing the effectiveness and accuracy of AI algorithms, this study aims to provide valuable tools for clinical decision-making and offers the potential to assist physicians and emergency care providers by delivering faster, more reliable predictions of HE, enabling timely interventions and leading to improved risk stratification, better prioritization of high-risk patients, and more effective resource allocation in emergency settings. Ultimately, this review focuses specifically on the role of AI in forecasting the risk of HE rather than diagnosing ICH or differentiating between types of ICHs.

## Methods

This systematic review and meta-analysis were conducted according to the Preferred Reporting Items for Systematic Reviews and Meta-Analyses (PRISMA) [18] guidelines. It is registered in the International Prospective Register of Systematic Reviews (PROSPERO) under the ID CRD42024627887.

### Search strategy

We searched PubMed, Embase, Scopus, and Web of Science databases to ensure no relevant articles were missed, the first 100 results from Google Scholar were reviewed as a supplementary search. The following search terms were included: (“expansion” OR “progression”) AND (“intra cerebral hematoma” or “ICH”) AND (“Artificial intelligence” OR “Machine learning” OR “Deep learning”). The described search strategy was applied to all aforementioned databases. The Medical Subject Headings (MeSH) and Emtree were used in PubMed and Embase, respectively, in combination with several similar keywords to develop the unique search strategy for each database. This search was performed from the inception of the respective databases until December 2, 2024. The full search strategy syntax for each database is outlined in Supplementary file 1 (Table S1).

### Inclusion criteria

1) English language, 2) Conducted on humans, 3) Involving patients with HE, 4) Reporting the use of ML and DL algorithms; including Random Forest (RF), Extreme Gradient Boosting (XGBoost), Categorical Boosting (CatBoost), Deep Neural Network (DNN), Random Neural Network (RNN), Chi-squared Automatic Interaction Detection (CHAID), Decision Tree (DT), Extreme Gradient Boosting (EGB), K-nearest neighbors (KNN), Support Vector Machine (SVM) in predicting poor outcomes, and 4) Original articles including cohort studies, randomized clinical trials, non-randomized clinical trials, observational case-series (> 20 cases), and case-control studies.

### Exclusion criteria

(1) Non-original articles, case reports, (2) Studies focusing on subarachnoid hemorrhages, subdural or epidural hematomas, or hematomas secondary to vascular malformations, aneurysms, tumors, or surgical complications (3) Hematomas with an unclear etiology or unspecified type (4) Hematomas occurring in pediatric populations or pregnant.

### Study selection

The extracted articles were added to EndNote version 21. According to the eligibility criteria, three reviewers (AN, SM and PP) independently evaluated the studies. Following the exclusion of duplicate records, screening was carried out in two phases: first, by examining the title and abstract, and then by selecting the most relevant studies for a full-text review. The investigations that satisfied the criteria for eligibility were selected for the phase of data extraction. In a dispute between three reviewers, a fourth reviewer (IM) participated.

### Data extraction

Two reviewers (AN and PP) separately extracted the intended data from included articles, including, first name, year of publication, country, number of patients, mean age, gender composition, design of the study, reference imaging study (e.g., digital subtraction angiography (DSA), computed tomography (CT), and magnetic resonance imaging (MRI)), ML and DL algorithm, sensitivity, specificity,

accuracy, precision, F1score, and AUC. The information from the articles was imported into a predesigned Excel sheet. HE, which was bolded as the main outcome, is considered in this data collection. Any discrepancies between the two reviewers were resolved through discussion, and if consensus was not reached, a third senior reviewer adjudicated the decision.

### Quality assessment

The PROBAST tool was used to evaluate the risk of bias (ROB) and the applicability of the included studies [19]. This tool evaluates four primary aspects: participants, predictors, results, and analysis. Each domain was assessed for risk of bias and categorized as low, high, or unclear risk. Additionally, the appropriateness of the forecasting models was evaluated within the same subject domains to determine if the research studies aligned with the research question.

### Statistical analysis

The metrics for true positives, true negatives, false positives, and false negatives for each high-performing algorithm in the included studies were collected for analysis. Sensitivity and specificity data were combined using a meta-analysis diagnostic model. Given the substantial heterogeneity across studies, all pooled estimates were calculated using random-effects models. All statistical analyses were conducted using the MIDAS package in STATA version 17.

## Results

### Study characteristics and selection process

In this systematic review, our initial search in the databases identified 1235 records. Duplicate records, including 179 papers, were removed. After an initial screening of titles and abstracts, 48 papers were chosen for additional assessment. Finally, 14 articles were included in the qualitative analysis, and meta-analysis, one of the studies included two different datasets with distinct outcomes, Since both datasets met the eligibility criteria for our study, we analyzed them as two separate studies [20]. The studies in our analysis were conducted across several countries. The PRISMA flow diagram showing the study selection process is provided in Fig. 1.

Altogether, the included studies comprised 7665 patients with a mean age of 58.7 years, of whom 41.26% were women. The mean time between the second CT scan and the initial CT scan was 36.92 h. Among all AI algorithms, 13 were DL and 10 were ML **(**Fig. 2**) (**Table 2**)**.

XGBoost was the best-performing algorithm with the highest average values for accuracy (0.9), sensitivity (0.62) and AUROC (0.96) followed by MLP; with accuracy of 0.92, sensitivity of 0.89, specificity of 0.92, and AUROC of 0.921 **(**Fig. 3**) (**Table 2**)**.

Among our included studies, the majority were from China (11 studies), while the remaining studies were from South Korea (2), Taiwan (1), and Spain (1). 10-fold cross-validation was utilized in 5 studies (35.7%), followed by 5-fold cross-validation in 4 studies (28.6%), while 5 studies (35.7%) did not report their validation method. All studies focused on CT-based radiomic features, with 6 studies (42.9%) using semi-automated methods, 5 studies (35.7%) employing automated methods, 2 studies (14.3%) relying on manual methods, and 1 study (7.1%) not specifying the extraction approach (Tables 1 and 2).

### Sensitivity and specificity

The analysis showed that the pooled sensitivity was 0.82 [95% CI: 0.74–0.88], with considerable heterogeneity ($I^2$ of 83.35%, p-value of 0). Regarding pooled specificity, the result was 0.83 [95% CI 0.78–0.87], with significant heterogeneity observed between the studies ($I^2$ of 88.04%, p-value of 0) (Fig. 4).

### Positive and negative diagnostic likelihood ratio (DLR)

The analysis showed a combined positive likelihood ratio of 4.91 [95% CI: 3.73–6.47], with a significant heterogeneity found among the studies (I2 value of 83.74%, p-value of 0). On the other hand, the pooled negative likelihood ratio was 0.21 [95% CI: 0.14–0.32], and there was notable heterogeneity observed between the studies (I2 value of 83.92%, p-value of 0) (Fig. 5).

### Diagnostic score and diagnostic odds ratio

The diagnostic score obtained from the pooled data was 3.14 [95% CI: 2.55–3.72], indicating significant heterogeneity (I2 of 99.29%, p-value of 0). The diagnostic odds ratio of the pooled data was 23.01 [95% CI: 12.83–41.24], with significant variation observed between the studies (I2 of 100%, p-value of $<0.001$) (Fig. 6).

### Area under curve

The pooled SROC curve, which combines sensitivity and specificity data, resulted in an AUC of 0.89 (95% CI: 0.86–0.92) (Fig. 7).

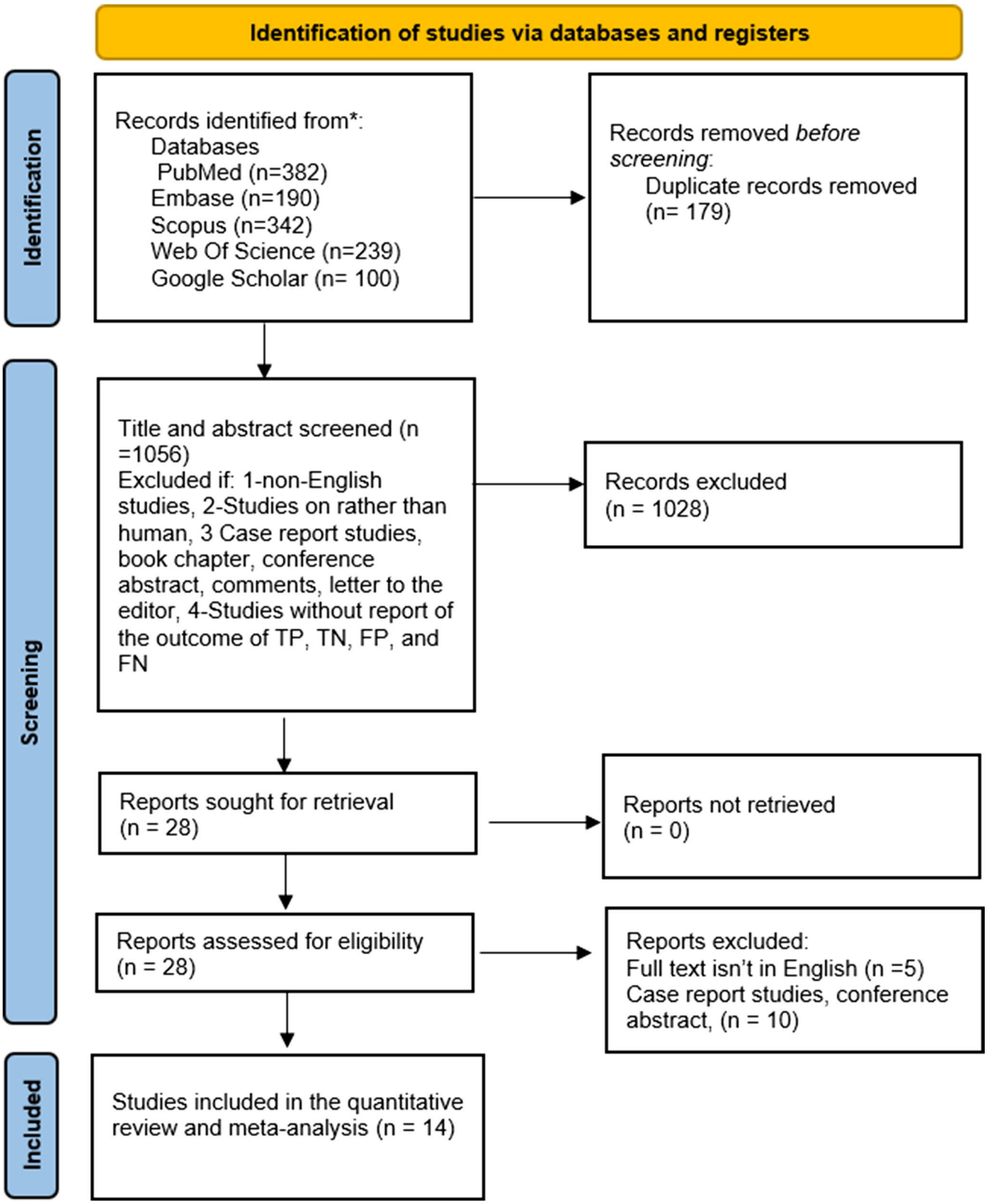


**Fig. 1** PRISMA flowchart of the study selection process

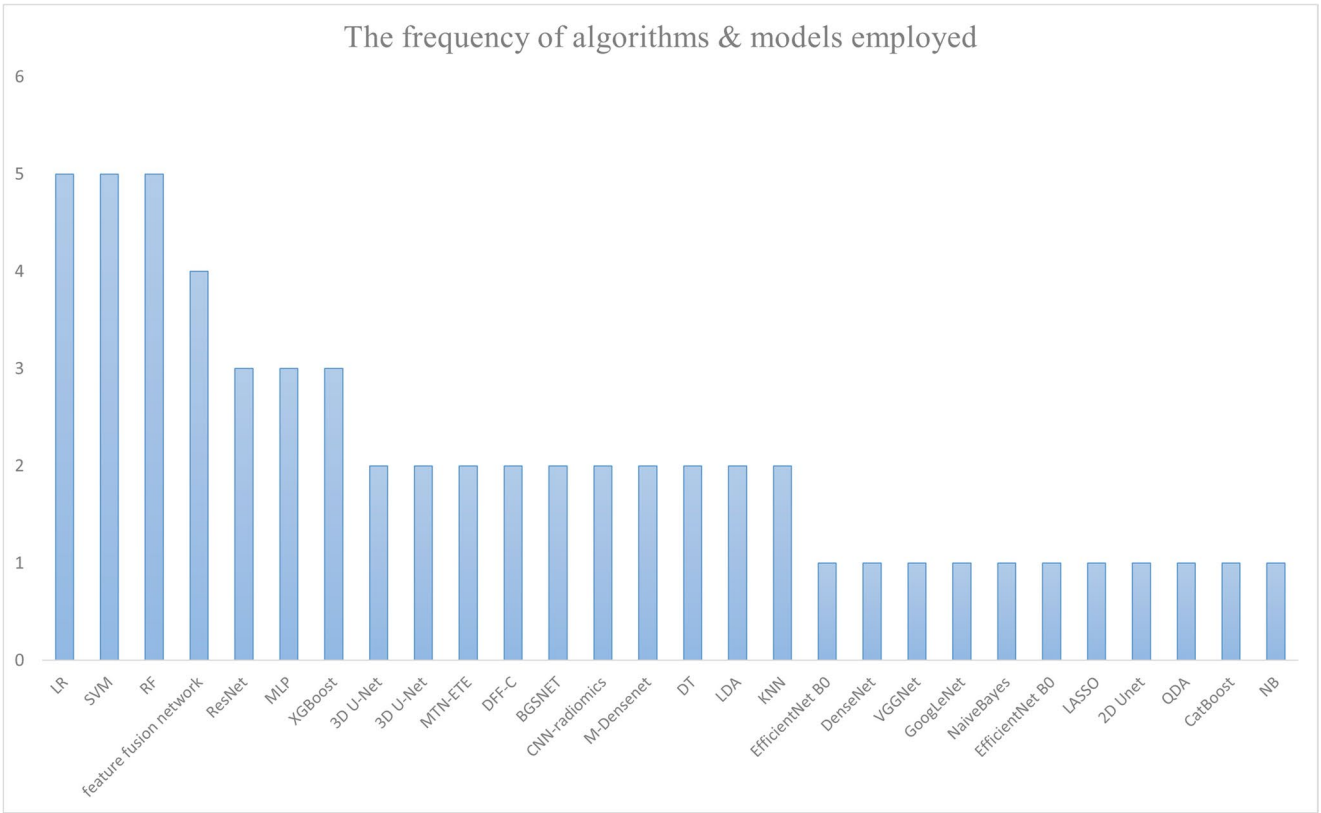


**Fig. 2** Frequency of algorithms used in the analyzed studies

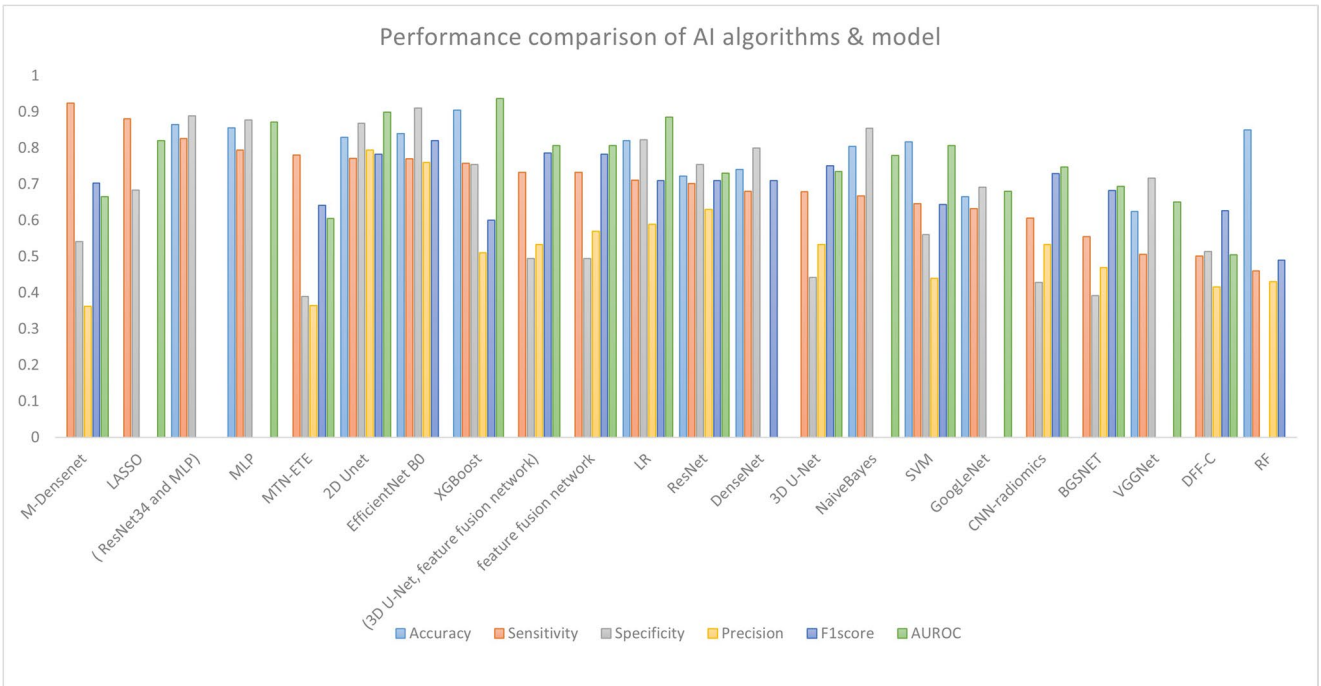


**Fig. 3** Performance comparison of ML algorithms, including accuracy, sensitivity, specificity and AUROC

**Table 1** Demographic and HE characteristics

| Author/year | Type of study | Country | progression criteria | Hematoma causes | Follow up CT (hr) | Mean age/female% | Inclusion criteria | Exclusion criteria |
|---|---|---|---|---|---|---|---|---|
| Xu et al. [38] | R | China | Hematoma volume increase>33% within 24 h | spontaneous | 24 | 62.7/68.3% | ICH within 6 h of symptom onset, Follow-up CT within 24 h, | Secondary causes of ICH, Poor-quality imaging, Surgery/intervention before follow-up CT |
| Cheng et al. [39] | R | China | a proportional increase of hematoma volume>33% or an absolute growth of hematoma volume>12.5 ml from baseline CT scans to follow-up CT scans | spontaneous | 48 | 59.64/35% | age>18 years; baseline CT scans performed within 6 h after ICH symptoms; ICH confirmed on NCCT showing parenchymal hematoma; follow-up CT scans performed within 48 h after the baseline CT scan | patients with secondary ICH caused by an arteriovenous malformation, cerebral aneurysm, traumatic brain injury, brain tumor, or hemorrhagic infarction and anticoagulant-associated ICH patients; patients who had surgical intervention before the follow-up CT scan |
| Chen et al. [24] | R | China | increase of 33% or 6mL in the hematoma volume from baseline to follow-up | spontaneous | 72 | 61.1/34% | patients aged>18 years with spontaneous ICH, Patients with baseline and follow-up cranial CT within 6 h and 72 h of symptom onset | traumatic ICH or hemorrhagic transformation of ischemic stroke, tumor, aneurysm or arteriovenous malformation presumed to be the potential cause of the bleeding, primary intraventricular hemorrhage or multiple ICH, usage of anticoagulant drugs prior to ictus, surgical intervention before the follow-up CT and severe artifacts on the original image |
| Zhang et al. [5] | R | China | follow-up CT scan showing 15% increase in size or number of hemorrhagic lesions, including newly developed ones | TBI | 12 | 54.9/23.9% | (1) brain contusion with intraparenchymal hemorrhage in CT scan, (2) brain contusions without evidence for neurological compromise, controlled ICP and no signifcant signs of mass efect on CT scan, (3) arrival at the emergency department within 12 h after injury and the frst head CT completed within 2 h after arrival; and (4) age≥18 years. | penetrating brain injury, combined epidural hematoma>10 ml, combined thickness of subdural hematoma>5 mm and/or a midline shift>5 mm and/or volume>10 ml, unilateral or bilateral loss of pupil reactivity or herniation syndrome, and pupil asymmetry of>2 mm |
| Y.-J. Shih et al. [6] | R | Taiwan | elative volume increase of more than 30% or an absolute volume increase of more than 10 mL compared to the initial CT. | TBI | 96 | 52.8/NA | Adults (≥18 years) with blunt TBI, Initial CT showing IPH, Follow-up CT within 96 h | Extra-axial hemorrhages only, Midline shift>5 mm, Herniation syndromes, Surgical intervention between CTs |

**Table 1** (continued)

| Author/year | Type of study | Country | progression criteria | Hematoma causes | Follow up CT (hr) | Mean age/female% | Inclusion criteria | Exclusion criteria |
|---|---|---|---|---|---|---|---|---|
| Q. Yang et al. [40] | R | China | the increase of the volume of intracranial hematoma by 25% or more when compared with the initial CT. The hematoma volume was calculated as ABC/2. | TBI | 6 | 58.14/79.71% | NA | patients<18 years old; patients with a history of skull surgery; patients with a baseline head CT more than 6 h after trauma; patients who did not undergo repeated CT within 3 days of baseline; severe artifacts on the baseline images; patients with penetrating TBI; (7) patients with brain surgery or interventional therapy before the follow-up head CT and patients with anticoagulant therapy before trauma; and patients with non-traumatic brain diseases, such as tumor, discovered on CT |
| Ko et al. [41] | R | South Korea | relative hematoma growth>33% or absolute hematoma growth>6 mL from baseline hemorrhage volume | spontaneous | 24 | 58.6/36% | primary spontaneous ICH with baseline volume≤60 mL, presentation to the emergency department within 6 h from symptom onset, availability of baseline and followup NCCT data within 48 h after symptom onset, and the absence of anticoagulant treatment | secondary ICH, hemorrhagic transformation of ischemic stroke, primary intraventricular hemorrhage, and NCCT images of insufficient quality |
| Li et al. [20] | R | China | absolute increase in hematoma volume of more than 6 mL on follow-up NCCT scans | spontaneous | 6–48 | 60.1/33.5% | ICH patients with or without hematoma expansion, Baseline and follow-up NCCT scans conducted within 6 h and 48 h from symptom onse | no follow-up NCCT, no hematoma, secondary ICH, poor preprocessoed NCCT |
| Li et al. [20] | P | China | absolute increase in hematoma volume of more than 6 mL on follow-up NCCT scans | spontaneous | 6–48 | 60.6/39% | ICH patients with or without hematoma expansion, Baseline and follow-up NCCT scans conducted within 6 h and 48 h from symptom onse | no follow-up NCCT, no hematoma, secondary ICH, poor preprocessoed NCCT |
| Wu et al. [31] | R | China | hematoma volume increases by >6mlor>33% compared with the initial hematoma volume at reexamination | spontaneous | 24 | NA/29.9% | age over 18 years old; conformed to the diagnostic criteria for cerebral hemorrhage; first CT examination and first CT reexamination both less than 24 h; the clinical data, complete imaging examination, and laboratory test results; and informed consent form of the patient | secondary cerebral hem-orrhage; implementing interventions such as surgery and intervention before CTreexamination; poor image quality, which affected judgment and measurement; and minimal cerebral hemorrhage (maximum diameter<3 mm) and multiple cerebral hemorrhage. |

**Table 1** (continued)

| Author/year | Type of study | Country | progression criteria | Hematoma causes | Follow up CT (hr) | Mean age/female% | Inclusion criteria | Exclusion criteria |
|---|---|---|---|---|---|---|---|---|
| Yalcin et al. [30] | R | Spain | NA | spontaneous | NA | NA | Patients older than 18 years; Diagnosis of acute spontaneous and anticoagulation associated supratentorial ICH within 12 h of symptom onset; Informed consent signed by the patient or relatives; Availability of both baseline and follow-up CTs for the calculation of volumetric differences in hematomas and label assignment; Baseline hematoma volume not less than 5 ml | Known secondary ICH etiology (trauma, underlying vascular malformation); Surgical hematoma evacuation; Life expectancy under 6 months; Pregnancy; Suboptimal imaging acquisition; Outlier cases based on IQR of baseline hematoma volume |
| C. Du et al. [42] | R | China | Hematoma volume increase>6 ml in follow-up CT | spontaneous | 24 | 59.4/46.0 | Baseline CT scan within 24 h and follow-up CT within 24 h; supratentorial hemorrhage | Secondary ICH, history of stroke, anticoagulant therapy, primary intraventricular hemorrhage |
| H. He et al. [33] | R | China | Hematoma volume increase>6 mL or >33% within 72 h | TBI | 72 | NA | Age≥18, 5-mm CT scan within 12 h post-trauma, Follow-up CT within 72 h, Clear traumatic intracerebral hematoma | Incomplete records, Severe CT artifacts, Pre-existing neurological deficits, Anticoagulant therapy |
| H. Lee et al. [34] | R | South Korea | A 20% or greater increase in the initial ICH area on follow-up CT scans within 12 h of the initial scan | TBI | NA | 57.2/28.5% | patients with mild to moderate traumatic brain injury (TBI), a Glasgow Coma Scale (GCS) score above 8, who had an initial non-contrast CT scan and did not require immediate neurosurgical intervention. | evere TBI (GCS score≤8) and patients requiring immediate neurosurgical intervention for acute subdural or epidural hematoma |
| F. Yu et al. [32] | R | China | Hematoma volume increase by >33% or >6 mL | spontaneous | 24 | 59.7/NA | patients with hypertension, who had their first CT scan within 24 h of disease onset, and a hemorrhage located in the brain parenchyma (including basal ganglia, thalamus, brain lobes, brainstem, or cerebellum). | patients with secondary ICH (due to trauma, cerebrovascular malformations, aneurysms, or tumors), ischemic cerebral infarction hemorrhagic transformation, those who underwent surgical treatment before CT examination, poor quality CT images, or hematomas with unclear borders preventing accurate ROI delineation. |

**Abbreviations**: NA: Not Applicated, R: Retrospective Study, P: Prospective Study, TBI: Traumatic Brain Injury, NCCT: Non-Contrast Computed Tomography, ICH: Intracerebral Hemorrhage, CT: Computed Tomography, hr: Hours, ICP: Intracranial Pressure, ROI: Region of Interest

**Table 2** AI algorithms characteristics and performance metrics

| Author/year | Validation | Type of reference Sequence | Input characteristics | Method of radiomics | No of extracted/final (radionics features) | No of patients in train/test group | AI algorithm & model | Best predictor | Accuracy | Sensitivity | Specificity | Precision | F1score | AUROC |
|---|---|---|---|---|---|---|---|---|---|---|---|---|---|---|
| Xu et al. [38] | 10 - fold cross - validation | CT | Radiomics (texture, shape) and imaging markers (satellite sign) | semi-automated | 396/4 | 68/61 | LASSO, LR | LR | NA | 0.95 | 0.766 | NA | NA | 0.857 |
| Cheng et al. [39] | 10 - fold cross - validation | CT | radiomics and clinical features | automated | 10/4 | 105/21 | ResNet34, MLP, VGGNet, GoogLeNet | combined (ResNet34 and MLP) | 0.865 | 0.826 | 0.889 | NA | NA | NA |
| Chen et al. [24] | 10 - fold cross- validation | CT | radiomics and clinical features | semi-automated | 15/3 | 864/289 | LASSO | LASSO | NA | 0.881 | 0.683 | NA | NA | 0.82 |
| Zhang et al. [5] | NA | CT | radiomics and clinical features | manual | NA | 66/22 | 2D Unet | 2D Unet | 0.829 | 0.771 | 0.868 | 0.794 | 0.783 | 0.899 |
| Y.-J. Shih et al. [6] | 10-fold cross-validation | CT | radiomics features and clinical features. | Manual | 107/NA | 107 | SVM, KNN | SVM | 0.776 | 0.622 | 0.887 | NA | NA | 0.76 |
| Q. Yang et al. [40] | 5-fold cross-validation | CT | radiomic features extracted from NCCT | semi-automated | 2017/12 | 145/62 | SVM, RF, LR, CatBoost, XGBoost | SVM | 0.806 | 0.818 | 0.793 | NA | 0.818 | 0.853 |
| Ko et al. [41] | NA | CT | radiomics | automated | NA | 197/50 | EfficientNet B0, DenseNet, ResNet | EfficientNet B0 | 0.84 | 0.77 | 0.91 | 0.76 | 0.82 | NA |
| Li et al. [20] | NA | CT | radiomics | automated | NA | 1876/608 | 3D U-Net, feature fusion network, MTN-ETE, DFF-C, BGSNET, CNN-radiomics, M-Densenet | combined two stages | NA | 0.784 | 0.666 | 0.663 | 0.711 | 0.767 |
| Li et al. [20] | NA | CT | radiomics | automated | NA | NA/500 | 3D U-Net, feature fusion network, MTN-ETE, DFF-C, BGSNET, CNN-radiomics, M-Densenet | combined two stages | NA | 0.646 | 0.8 | 0.326 | 0.354 | 0.806 |
| Wu et al. [31] | NA | CT | radiomics and clinical features | automated | NA | 204/50 | MLP, Naive-Bayes, LR | MLP | 0.92 | 0.889 | 0.927 | NA | NA | 0.921 |
| Yalcin et al. [30] | 5-fold cross-validation | CT | radiomics | semi-automated | NA | 73/24 | EfficientNet B0, DenseNet, ResNet | EfficientNet B0 | 0.84 | 0.77 | 0.91 | NA | 0.82 | NA |
| C. Du et al. [42] | NA | CT | Clinical features and radiomics (CT markers) | Manual | NA | NA | XGBoost, SVM, RF, LR | XGBoost | 0.9 | 0.62 | NA | 0.51 | 0.6 | 0.96 |
| H. He et al. [33] | 5-fold cross-validation | CT | Radiomics (CT-based) and clinical features | Semi-automatic | 1,502/7 | 315/137 | LR, SVM, RF, LDA, DT | LR | 0.797 | 0.744 | 0.861 | NA | 0.8 | 0.848 |
| H. Lee et al. [34] | NA | CT | Radiological+clinical | manually extracted radiological features | 7/7 | 520/65 | XGBoost, RF | XGBoost | 0.91 | 0.8958 | 0.7549 | NA | NA | 0.913 |
| F. Yu et al. [32] | 10-fold cross-validation | CT | Radiomics+clinical+conventional imaging feature | Semi-automated | 1218/29 | 555/77 | LR, KNN, SVM, DT, RF, LDA, QDA, NB | LR | 0.883 | 0.85 | 0.894 | 0.739 | 0.791 | 0.917 |

**Abbreviations**: NA: Not Applicated, CT: Computed Tomography, NCCT: Non-Contrast Computed Tomography, MLP: Multi-Layer Perceptron, SVM: Support Vector Machine, RF: Random Forest, LR: Logistic Regression, LASSO: Least Absolute Shrinkage and Selection Operator, KNN: K-Nearest Neighbors, AUROC: Area Under the Receiver Operating Characteristic Curve, F1score: F1 Score, ResNet: Residual Network, VGGNet: Visual Geometry Group Network, CNN: Convolutional Neural Network, 2D Unet/3D Unet: Two-/Three-Dimensional U-Net Model, XGBoost: Extreme Gradient Boosting, LDA: Linear Discriminant Analysis, DT: Decision Tree, QDA: Quadratic Discriminant Analysis, EfficientNet: Efficient Convolutional Neural Network Model

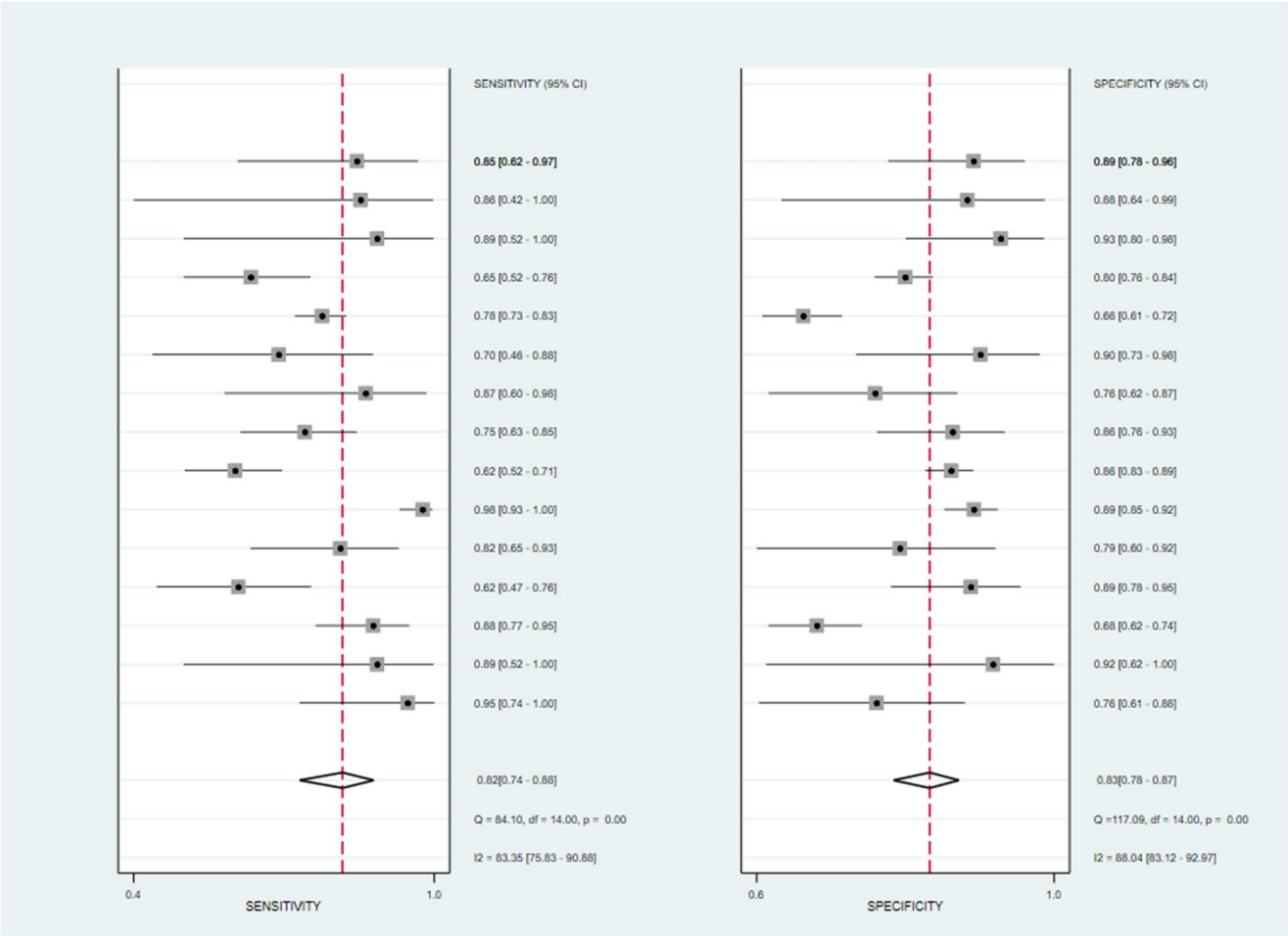


**Fig. 4** Sensitivity and specificity of ML algorithms

## Sub-group between TBI (Traumatic brain Injury) and spontaneous

Among the 14 included studies, 5 studies (35.7%) focused on TBI, while the remaining 9 studies (64.3%) investigated spontaneous ICH. Regarding the total 7,665 patients, 1,925 patients (25.1%) had TBI-associated ICH, whereas the remaining 5,740 patients (74.9%) belonged to the spontaneous ICH subgroup.

The comparison between ICH, HE following TBI, and spontaneous subgroups revealed that the spontaneous group demonstrated superior diagnostic performance with a higher AUROC (0.90 vs. 0.87), sensitivity (0.85 vs. 0.76), and diagnostic odds ratio (28 vs. 16). Specificity was comparable between the two groups (0.83 in both). The spontaneous group also showed a lower negative likelihood ratio (0.18 vs. 0.29), indicating better exclusion of false negatives. However, the spontaneous subgroup exhibited significant heterogeneity ($I^2$ = 96%), while the TBI subgroup had no heterogeneity ($I^2$ = 0%), suggesting variability in the spontaneous ICH studies.

## Publication bias assessment

The regression-based analysis estimated the bias coefficient at 6.85 (95% CI: −13.84 to 27.54, $P$=0.487), showing no statistically significant bias. The wide confidence interval suggests uncertainty in the estimate. However, the intercept of 2.52 (95% CI: 0.86 to 4.18, $P$=0.006) was statistically significant, potentially indicating some degree of bias despite the lack of strong evidence for small-study effects.

A Deeks' test for funnel plot asymmetry showed no significant publication bias, with a P-value of 0.49. Visual inspection and the regression line confirmed no substantial small-study effects, indicating that the studies in the meta-analysis were not influenced by selective reporting (Fig.S1).

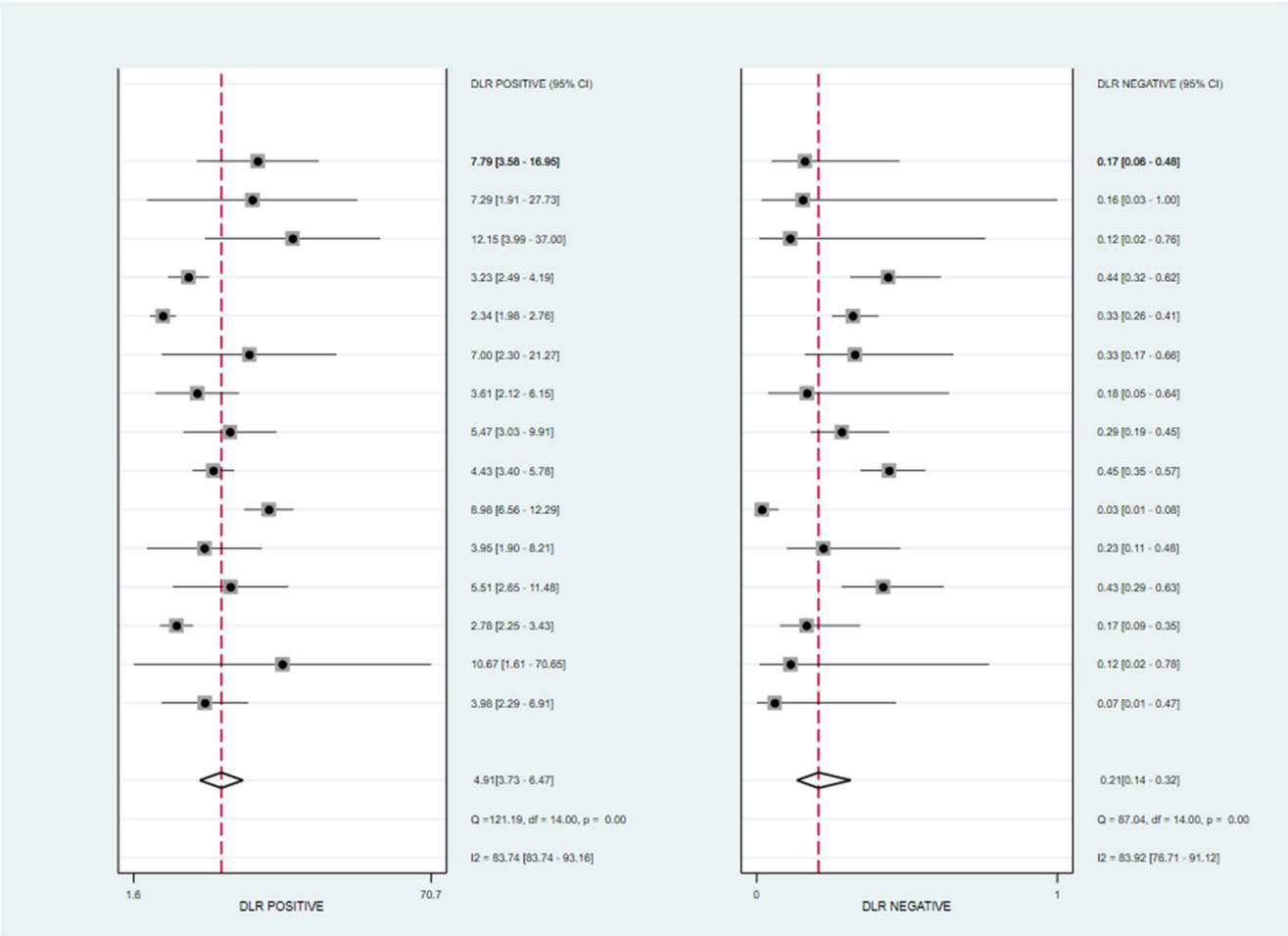


**Fig. 5** Positive and negative DLR of ML algorithms

## Risk of bias (PROBAST)

Across the four domains of participants, predictors, outcomes, and analysis, 93% of studies demonstrated low risk of bias. In 7% of studies, the ROB was unclear, particularly in the predictor and analysis domains. No studies were rated as having a high ROB **(**Fig.S2).

## Applicability of the ML tools (PROBAST)

For applicability, 94% of studies showed low concern in the participants domain, and 92% in the predictor domain. Similarly, 93% of studies demonstrated low concern in the outcome's domain, and 95% in the analysis domain. A small percentage (6–8%) across domains was classified as unclear. No domains were noted as having high concern (Fig.S3).

# Discussion

The application of AI-based models to predict HE in ICH represents a promising advancement in neurocritical care. This systematic review and meta-analysis evaluated the current evidence on the predictive performance of AI-based models in this regard. The pooled sensitivity of 82% [95% CI: 74–88%] shows that AI models can accurately identify most cases of HE, thus decreasing the chances of missed diagnosis and enabling early interventions. Moreover, the pooled specificity of 83% [95% CI: 78–87%] indicates that these models can also exclude non-HE cases effectively, which reduces false positives and unnecessary treatments. The positive DLR of 4.91 [95% CI: 3.73–6.47] indicates that when the prediction is positive, this will increase the odds of HE by almost fivefold. On the other hand, the

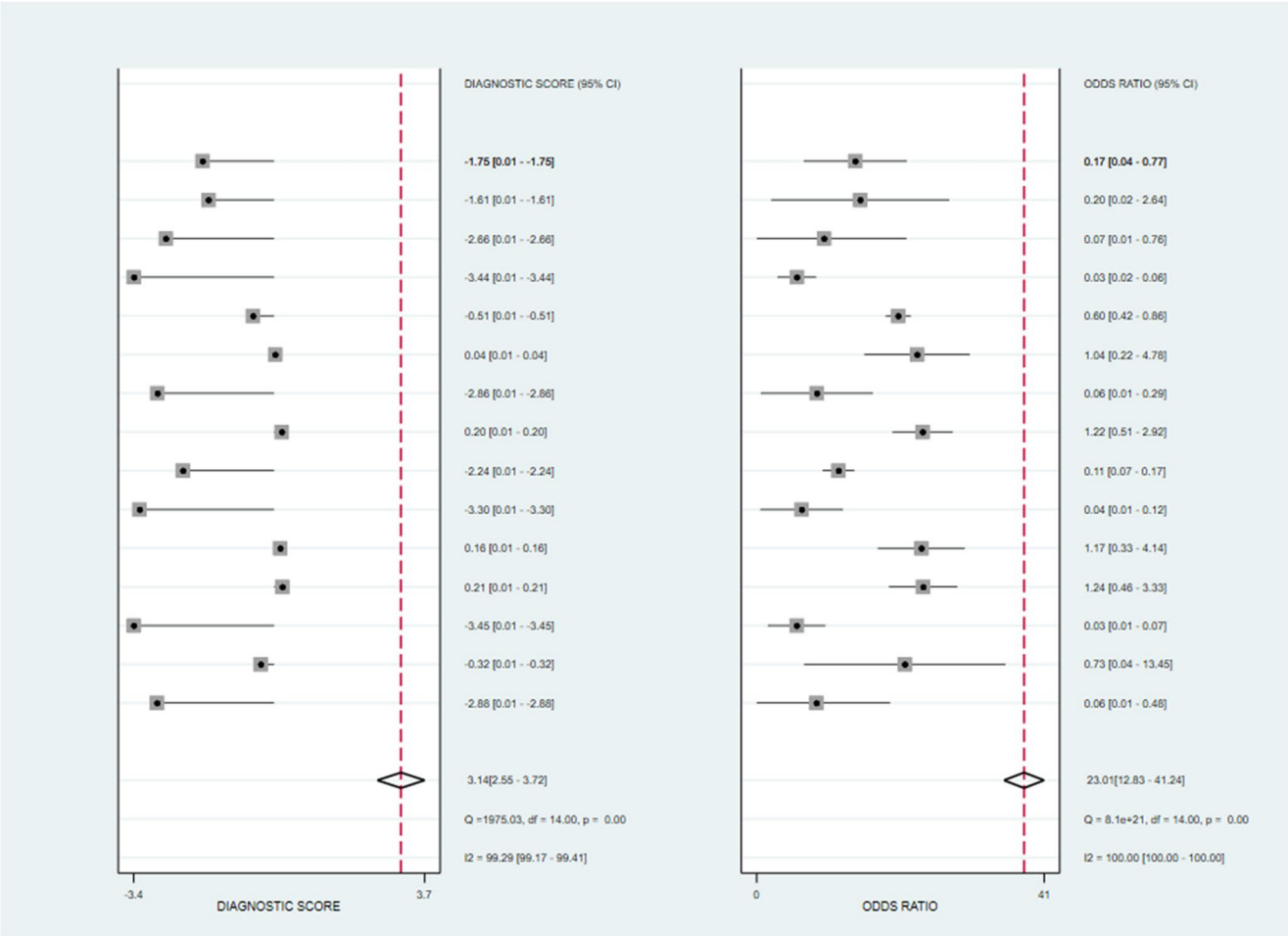


**Fig. 6** Diagnostic score and diagnostic odds ratio of ML algorithms

negative DLR of 0.21 [95% CI: 0.14–0.32] significantly reduced the probability of having an HE when the prediction is negative. Further, the DOR of 23.01 [95% CI: 12.83–41.24] pools sensitivity and specificity, reflecting the strong overall diagnostic accuracy of AI systems. Finally, the AUC of 0.89 [95% CI: 0.86–0.92] underlines the high discriminatory capability of AI-based models, supporting their clinical utility in forecasting HE and aiding critical decision-making in managing ICH patients.

Several nomograms and AI-based radiomics models have been developed to predict the HE following ICH [21–24]. Yang et al. developed a LR-based nomogram for predicting HE after ICH, identifying baseline hematoma ≥ 20 mL (OR: 4.09) and time to CT < 1 h (OR: 4.19) as key predictors [21]. Zhang et al. developed an LR-based nomogram to predict HE [22]. They showed that the National Institutes of Health Stroke Scale (NIHSS) and International Normalized Ratio (INR) were the most significant predictive factors, followed by time to baseline CT scan, CTA spot signs, and hypodensities [22]. Their model showed a sensitivity of 74% and specificity of 64% with a C-index of 0.743 [22].

Despite promising predictive outcomes of nomograms concurrent with their straightforward interpretation and daily application, These models rely on limited parameters and cannot adequately handle large datasets with multiple variables [22]. In contrast, AI-based models can analyze datasets with substantial sample sizes and identify the correlation between clinical, treatment, and radiological variables [23]. The AI-based models have demonstrated an AUC and ACC ranging from 0.5 to 0.96 and 0.624 to 0.92, respectively, which indicate these models' favorable predictive performance in HE prediction [2, 21, 22, 25–29]. Recently, the prediction of HE using only the initial scan has drawn increasing attention in research. CT imaging markers such as the island sign, hypodensity, satellite sign, black hole sign, blend sign, and swirl sign have been proposed as indicators of HE [30].

Using DL models based on admission NCCT scans, C. Yalcin et al. modeled a deep learning framework that leverages the 2D EfficientNet B0 model to predict HE. This image-ba3sed approach demonstrated superior performance compared to models like DenseNet121 and ResNet34. By

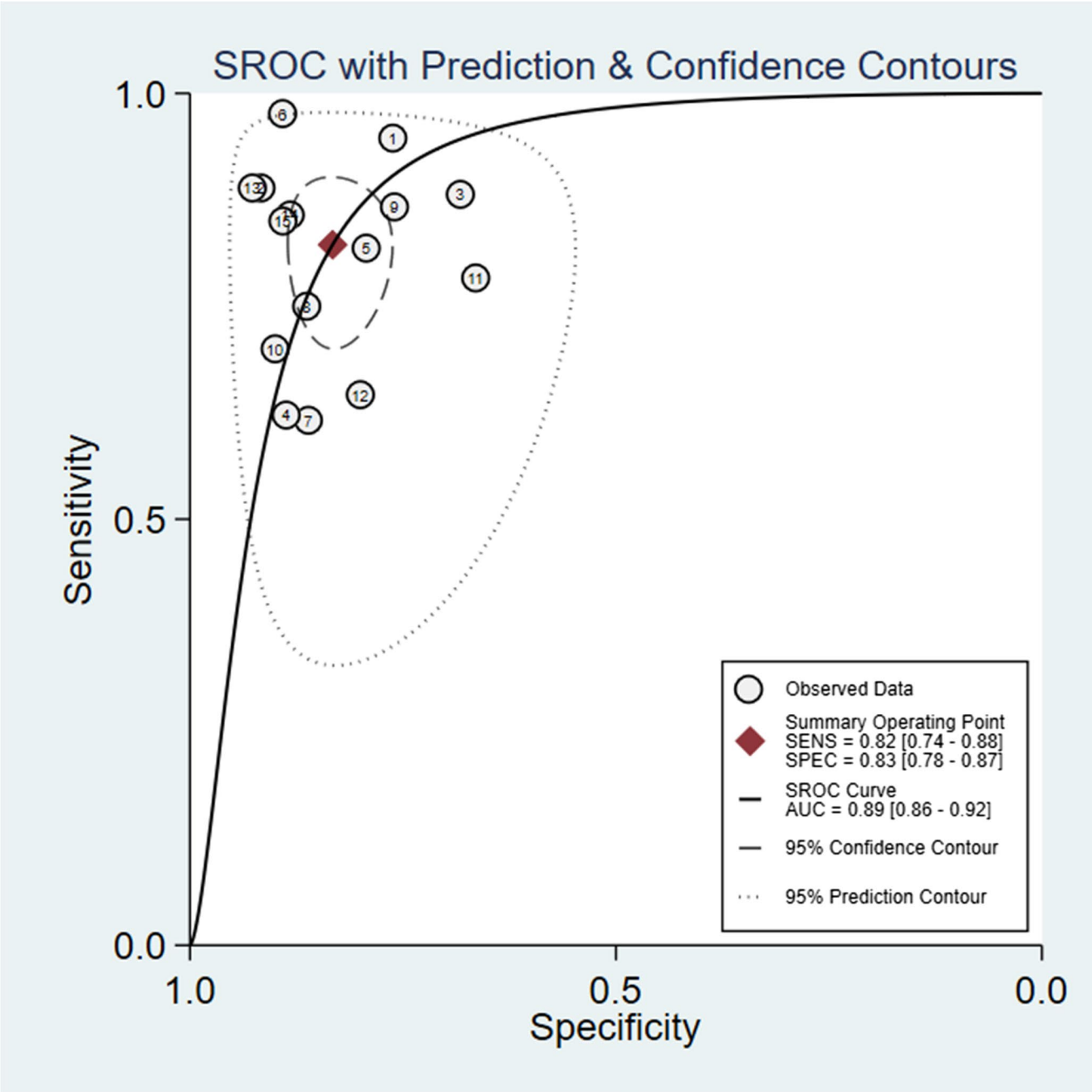


**Fig. 7** Summary receiver operator characteristic curve (SROC) of ML algorithms

incorporating synthetic images alongside standard data augmentation techniques to tackle dataset and disease-related challenges, the model achieved remarkable results with an accuracy of 0.84, an F1-score of 0.82, a sensitivity of 0.77, and a specificity of 0.91 [30].

In another approach, Li et al. developed non-automatic and automatic approaches. The first phase utilized a multi-task 3D U-Net to segment hematomas and generate preliminary risk scores, leveraging hematoma segmentation for multi-scale feature learning in HE prediction. The second phase employed a feature fusion network to refine the risk score by integrating deep features from the first phase and hematoma mask-derived features (i.e., radiomics properties and hematoma volume). AUC results show 0.767 in the first phase and 0.760 in the second. Non-automatic methods show limited performance, while CNN-radiomics achieves the highest sensitivity (0.840) but low specificity (0.558). Conversely, M-Densenet121 favors specificity over sensitivity [20].

Wu et al. utilized a joint model integrating clinical and imaging data with the VGG deep learning framework,

achieving superior predictive performance among MLP models, with a test accuracy of 0.920, and AUC scores of 0.921 [31]. The VGG-19 model is utilized for feature extraction from images, leveraging its deep convolutional layers to capture complex patterns. These extracted features are then used as input for various ML models such as LR, SVM, and RF, which are employed for validation and prediction tasks. This combination enhances the predictive accuracy by integrating deep learning and traditional ML methods.

Similarly, F. Yu et al. developed a nomogram integrating clinical data and imaging signs to assess HE risk in HICH patients. Various ML algorithms (LR, KNN, SVM, DT, RF, LDA, QDA, NB) achieved training set AUCs ranging from 0.788 to 1.000, with 10-fold cross-validation AUCs averaging between 0.645 and 0.845. The LR algorithm, considered the most stable, was used for constructing the radiomics model, achieving an AUC of 0.827 in the validation set. Key predictors—admission GCS score, hematoma volume, irregular shape, and Rad score—were identified via multivariate LR to create a hybrid model. This model achieved AUCs of 0.901, 0.838, and 0.917 in the training, validation, and test sets, respectively [32].

A three-dimensional (3D) segmentation network for the semi-automatic segmentation of traumatic intracerebral hematomas was developed based on the open-source SSL4MIS segmentation model to train popular 3D convolutional encoder-decoder networks, including 3DUNet, Attention-3DUNet, and 3DVNet. Attention-3DUNet was utilized as an assistance in segmentation to ease physicians' workload, minimize manual variations, and improve consistency. Integrated radiomic and clinical features achieved the best performance (AUC = 0.83), outperforming radiomic models (AUC = 0.8) and clinical models (AUC = 0.77) in predicting hematoma expansion [33].

In the first application of an ML model to predict HE in traumatic brain injury (TBI), LR achieved a promising AUC of 0.82. However, the SHAP value-enhanced XGBoost model significantly surpasses it with an AUC of 0.913. SHAP values improve the interpretability of individual risk factors, providing clinicians with a powerful tool for personalized analysis of ICH progression and enabling more precise, tailored decision-making [34].

## Clinical implications

The clinical applicability of AI-based models for predicting hematoma expansion remains promising but faces important barriers. A major challenge is the lack of standardized imaging protocols, as variations in acquisition parameters and modalities (CT, CTA, MRI) can significantly affect reproducibility and model performance. Automated and reliable segmentation of hematomas is another critical requirement, since manual methods are time-consuming and subject to inter-observer variability. Furthermore, most AI models operate as "black boxes," limiting interpretability and potentially reducing clinicians' trust in their predictions. For successful integration into clinical workflows, these models must undergo rigorous external validation across diverse populations and healthcare systems, and they should be embedded within user-friendly platforms that can interact with hospital information systems. Collaboration between clinicians, radiologists, and data scientists will be essential to ensure that AI models are not only technically accurate but also clinically meaningful and feasible for real-world application.

## Limitation

Despite the promising predictive outcomes of AI-based models, these novel tools are correlated with various limitations. Dependency on high-quality, large datasets for training is a major limitation for AI models, especially in neurosurgical fields, due to the rarity and heterogeneity of conditions [35]. Poor generalizability due to the overfitting of models, especially when trained on small datasets, is another limitation of the application of AI models in neurosurgery [36]. The lack of standardized metrics, imaging protocol inconsistencies, and variability in data labeling are other limitations of AI-based models that limits their reproducibility and external validation [37]. These limitations highlight that the results of the AI models should be interpreted meticulously. In addition, the included studies used heterogeneous definitions of hematoma expansion (e.g., absolute increase >6 mL vs. relative increase >33%), which may have influenced the pooled results and contributed to the high heterogeneity observed. Standardized definitions of HE will therefore be essential for future studies to allow more reliable comparisons and meta-analyses. these limitations highlight that the results of the AI models should be interpreted meticulously.

## Future directions

To enhance the clinical applicability and performance of AI-based models in predicting HE in ICH, future studies should aim at increasing the diversity and size of patient datasets, integrating multi-center prospective research to enrich model robustness. Larger cohorts and more varied populations will help in addressing the potential biases of small-scale studies, ensuring that predictive models are both accurate and widely applicable.

In addition, developing standardized imaging protocols, particularly for MRI and CT scans, will be critical for improving the reproducibility and generalizability of AI models. Variations in imaging techniques and feature extraction methods have contributed to inconsistencies in

current studies, emphasizing the need for a unified approach across research centers.

Furthermore, exploring a broader range of machine learning algorithms, especially deep learning models, could help refine model predictions. Optimizing these models for different ICH subtypes, such as traumatic versus spontaneous hemorrhage, would enhance their specificity and sensitivity.

External validation using independent multi-center cohorts is also essential to confirm the robustness of AI predictions and facilitate their integration into routine clinical practice. Ensuring that these models generalize well across diverse patient populations will be crucial for translating AI advancements into tangible clinical outcomes, enabling timely and personalized interventions in ICH management.

## Conclusion

This study highlights the potential of AI models, particularly ML and DL, in predicting HE in ICH. The pooled sensitivity (0.82), specificity (0.83), and AUC (0.89) indicate a potentially useful diagnostic performance; however, the high heterogeneity across studies limits the robustness of these findings. Subgroup analysis suggested better outcomes in predicting spontaneous ICH compared to traumatic ICH. While the results are encouraging, variability in imaging protocols and feature extraction methods restricts generalizability. Therefore, standardized imaging protocols and rigorous external validation are essential before AI-based models can be reliably integrated into clinical practice.

**Supplementary Information** The online version contains supplementary material available at https://doi.org/10.1007/s10143-025-03901-7.

**Acknowledgements** Nothing to acknowledge.

**Author contributions** The conception and design of the study: Ibrahim Mohammadzadeh (IM), Pascal Jabbour (PJ) and Ahmet Günkan (AG). Acquisition of data: Amin Mohamad Niaei, Paniz Sanjari Pirayvatloo. Analysis and interpretation of data: IM and (AG). Drafting the article: IM, Bardia Hajikarimloo (BH) and Mohammad Amin Habibi (MAH). Revising it critically for important intellectual content: AG, Shahin Mohammadzadeh, PJ, Adam A Dmytriw, PM and BH. Final approval of the version to be submitted: All authors.

**Funding** The authors did not receive support from any organization for the submitted work.

**Data availability** The data that support the findings of this study are available from the corresponding author, I. Mohammadzadeh, upon reasonable request.

## Declarations

**Ethical approval** The study is deemed exempt from receiving ethical approval.

**Consent to participate** Not applicable.

**Originality and exclusivity** Not applicable. The manuscript is original and has not been published or submitted elsewhere.

**Competing interests** The authors declare no competing interests.

**Clinical trial number** Not applicable.

**Compliance with instructions** The authors confirm the manuscript follows all journal guidelines.

**Reporting checklist** The manuscript follows the PRISMA checklist. The checklist has been submitted.

## References

1. An SJ, Kim TJ, Yoon BW, Epidemiology (2017) Risk Factors, and clinical features of intracerebral hemorrhage: an update. J Stroke 19(1):3–10 (In eng). https://doi.org/10.5853/jos.2016.00864
2. Liu J, Xu H, Chen Q et al (2019) Prediction of hematoma expansion in spontaneous intracerebral hemorrhage using support vector machine. EBioMedicine 43:454–459. https://doi.org/10.1016/j.ebiom.2019.04.040
3. Mohammadzadeh I, Niroomand B, Tajerian A, Shahnazian Z, Nouri Z, Mortezaei A (2024) Coagulopathy at admission in traumatic brain injury and its association with hematoma progression: a systematic review and meta-analysis of 2,411 patients. Clin Neurol Neurosurg 108699
4. Li N, Ding S, Liu Z et al (2025) A deep learning-based framework for predicting intracerebral hematoma expansion using head non-contrast CT scan. Acad Radiol 32(1):347–358. https://doi.org/10.1016/j.acra.2024.07.039
5. Zhang L, Zhuang Q, Wu G et al (2022) Combined radiomics model for prediction of hematoma progression and clinical outcome of cerebral contusions in traumatic brain injury. Neurocrit Care. 11:1–11 https://doi.org/10.1007/s12028-021-01320-2
6. Shih Y-J, Liu Y-L, Chen J-H et al (2022) Prediction of intraparenchymal hemorrhage progression and neurologic outcome in traumatic brain injury patients using radiomics score and clinical parameters. Diagnostics 12(7):1677
7. Haider SP, Qureshi AI, Jain A et al (2023) Radiomic markers of intracerebral hemorrhage expansion on non-contrast CT: independent validation and comparison with visual markers. Front Neurosci 17:1225342
8. Brouwers HB, Greenberg SM (2013) Hematoma expansion following acute intracerebral hemorrhage. Cerebrovasc Dis 35(3):195–201
9. Davis S, Broderick J, Hennerici M et al (2006) Hematoma growth is a determinant of mortality and poor outcome after intracerebral hemorrhage. Neurology 66(8):1175–1181
10. Gilotra K, Swarna S, Mani R, Basem J, Dashti R (2023) Role of artificial intelligence and machine learning in the diagnosis of cerebrovascular disease. Front Hum Neurosci 17:1254417
11. Mohammadzadeh I, Niroomand B, Shahnazian Z et al (2024) Machine learning for predicting poor outcomes in aneurysmal subarachnoid hemorrhage: a systematic review and meta-analysis involving 8,445 participants. Clin Neurol Neurosurg 108668
12. Mohammadzadeh I, Niroomand B, Eini P, Khaledian H, Choubineh T, Luzzi S (2025) Leveraging machine learning algorithms to forecast delayed cerebral ischemia following subarachnoid hemorrhage: a systematic review and meta-analysis of 5,115 participants. Neurosurg Rev 48(1):26. https://doi.org/10.1007/s10143-024-03175-5

13. Mohammadzadeh I, Niroomand B, Hajikarimloo B et al (2025) Can we rely on machine learning algorithms as a trustworthy predictor for recurrence in High-Grade glioma? A systematic review and meta-analysis. Clin Neurol Neurosurg. https://doi.org/10.1016/j.clineuro.2025.108762
14. Mohammadzadeh I, Hajikarimloo B, Niroomand B et al (2025) Application of artificial intelligence in forecasting survival in high-grade glioma: systematic review and meta-analysis involving 79,638 participants. Neurosurg Rev 48(1):1–13
15. Khan OR, Farooqi HA, Nabi R, Hasan H (2024) Advancements in prognostic markers and predictive models for intracerebral hemorrhage: from serum biomarkers to artificial intelligence models. Neurosurg Rev 47(1):382
16. Liu J, Xu H, Chen Q et al (2019) Prediction of hematoma expansion in spontaneous intracerebral hemorrhage using support vector machine. EBioMedicine 43:454–459
17. Zhao K, Zhao Q, Zhou P, Liu B, Zhang Q, Yang M (2022) Can artificial intelligence be applied to diagnose intracerebral hemorrhage under the background of the fourth industrial revolution? A novel systemic review and meta-analysis. Int J Clin Pract 2022(1):9430097
18. Page MJ, McKenzie JE, Bossuyt PM et al (2021) The PRISMA 2020 statement: an updated guideline for reporting systematic reviews. bmj 372
19. Wolff RF, Moons KG, Riley RD et al (2019) PROBAST: a tool to assess the risk of bias and applicability of prediction model studies. Ann Intern Med 170(1):51–58
20. Li N, Ding S, Liu Z et al (2024) A deep learning-based framework for predicting intracerebral hemorrhage hematoma expansion using head Non-contrast CT scan. Acad Radiol
21. Yang M, Du C, Zhang Q, Ma Q, Li R (2020) Nomogram model for predicting hematoma expansion in spontaneous intracerebral hemorrhage: multicenter retrospective study. World Neurosurg 137:e470–e478. https://doi.org/10.1016/j.wneu.2020.02.004
22. Zhang C, Ge H, Zhong J et al (2020) Development and validation of a nomogram for predicting hematoma expansion in intracerebral hemorrhage. J Clin Neurosci 82:99–104. https://doi.org/10.1016/j.jocn.2020.10.027
23. Ye H, Jiang Y, Wu Z et al (2024) A comparative study of a nomogram and machine learning models in predicting early hematoma expansion in hypertensive intracerebral hemorrhage. Acad Radiol 31(12):5130–5140. https://doi.org/10.1016/j.acra.2024.05.035
24. Chen Q, Zhu D, Liu J et al (2021) Clinical-radiomics nomogram for risk estimation of early hematoma expansion after acute intracerebral hemorrhage. Acad Radiol 28(3):307–317
25. Jiang Y-W, Xu X-J, Wang R, Chen C-M (2023) Efficacy of non-enhanced computer tomography-based radiomics for predicting hematoma expansion: a meta-analysis. Front Oncol. https://doi.org/10.3389/fonc.2022.973104
26. Li Q, Zhang G, Huang Y-J et al (2015) Blend sign on computed tomography: novel and reliable predictor for early hematoma growth in patients with intracerebral hemorrhage. Stroke 46(8):2119–2123
27. Li Q, Zhang G, Xiong X et al (2016) Black hole sign: novel imaging marker that predicts hematoma growth in patients with intracerebral hemorrhage. Stroke 47(7):1777–1781
28. Shakya MR, Fu F, Zhang M et al (2021) Comparison of black hole sign, satellite sign, and iodine sign to predict hematoma expansion in patients with spontaneous intracerebral hemorrhage. BioMed Res Int 2021(1):3919710
29. Zhou L, Jiang Z, Tan G, Wang Z (2021) A meta-analysis of the predictive significance of the Island sign for hematoma expansion in intracerebral hemorrhage. World Neurosurg 147:23–28
30. Yalcin C, Abramova V, Terceño M, Oliver A, Silva Y, Lladó X (2024) Hematoma expansion prediction in intracerebral hemorrhage patients by using synthesized CT images in an end-to-end deep learning framework. Comput Med Imaging Graph 117:102430
31. Wu F, Wang P, Yang H et al (2024) Research on predicting hematoma expansion in spontaneous intracerebral hemorrhage based on deep features of the VGG-19 network. Postgrad Med J. https://doi.org/10.1093/postmj/qgae037
32. Yu F, Yang M, He C et al (2024) CT radiomics combined with clinical and radiological factors predict hematoma expansion in hypertensive intracerebral hemorrhage. Eur Radiol. 1–14. https://doi.org/10.1007/s00330-024-10921-2
33. He H, Liu J, Li C et al (2024) Predicting hematoma expansion and prognosis in cerebral contusions: a radiomics-clinical approach. J Neurotrauma. https://doi.org/10.1089/neu.2023.0410
34. Lee HS, Kim JH, Son J, Park H, Choi J (2024) Machine learning models for predicting early hemorrhage progression in traumatic brain injury. Sci Rep 14(1):11690
35. Iqbal MS, Heyat MBB, Parveen S et al (2024) Progress and trends in neurological disorders research based on deep learning. Comput Med Imaging Graph. https://doi.org/10.1016/j.compmedimag.2024.102400
36. Chang K (2020) Enhancing medical imaging workflows with deep learning. Massachusetts Institute of Technology
37. Fedorov A, Longabaugh WJ, Pot D et al (2023) National cancer Institute imaging data commons: toward transparency, reproducibility, and scalability in imaging artificial intelligence. Radiographics 43(12):e230180
38. Xu W, Ding Z, Shan Y et al (2020) A nomogram model of radiomics and satellite sign number as imaging predictor for intracranial hematoma expansion. Front Neurosci 14:491
39. Cheng X, Zhang W, Wu M et al (2021) A prediction of hematoma expansion in hemorrhagic patients using a novel dual-modal machine learning strategy. Physiol Meas 42(7):074005
40. Yang Q, Sun J, Guo Y et al (2022) Radiomics features on computed tomography combined with clinical-radiological factors predicting progressive hemorrhage of cerebral contusion. Front Neurol 13:839784
41. Ko DR, Na H, Jung S, Lee S, Jeon J, Ahn SJ (2024) Hematoma expansion prediction in patients with intracerebral hemorrhage using a deep learning approach. J Med Artif Intell. https://doi.org/10.21037/jmai-24-5
42. Du C, Li Y, Yang M, Ma Q, Ge S, Ma C (2024) Prediction of hematoma expansion in intracerebral hemorrhage in 24 hours by machine learning algorithm. World Neurosurg 185:e475–e483

## Authors and Affiliations

**Ibrahim Mohammadzadeh[1] · Bardia Hajikarimloo[2] · Shahin Mohammadzadeh[1] · Amin Mohamad Niaei[3] · Paniz Sanjari Pirayvatloo[4] · Mohammad Amin Habibi[5] · Poriya Minaee[1] · Adam A. Dmytriw[6] · Ahmet Günkan[7] · Pascal Jabbour[8]**

✉ Ibrahim Mohammadzadeh
ibrahim.mohammadzadeh@sbmu.ac.ir; Ibrahim.mdz7777@gmail.com

✉ Pascal Jabbour
Pascal.Jabbour@jefferson.edu

Bardia Hajikarimloo
kjh7vp@uvahealth.org

Shahin Mohammadzadeh
shahinmdz1381@gmail.com

Amin Mohamad Niaei
amin.niaei79@gmail.com

Paniz Sanjari Pirayvatloo
Sanjarip82@gmail.com

Mohammad Amin Habibi
Mohammad.habibi1392@yahoo.com

Poriya Minaee
Poriyaporiya0@gmail.com

Adam A. Dmytriw
adam.dmytriw@gmail.com

Ahmet Günkan
gunkanahmet@gmail.com

1 Skull Base Research Center, Loghman-Hakim Hospital, Shahid Beheshti University of Medical Sciences, Tehran, Iran

2 Department of Neurological Surgery, University of Virginia, Charlottesville, VA, USA

3 School of Medicine, Lorestan university of medical sciences, Lorestan, Iran

4 Student Research Committee, School of Medicine, Iran University of Medical Science, Tehran, Iran

5 Department of Neurosurgery, Shariati Hospital, Tehran University of Medical Sciences, Tehran, Iran

6 Neuroendovascular Program, Women's Hospital, Massachusetts General Hospital & Brigham, Harvard Medical School, Boston, MA, USA

7 Division of Vascular and InterventionalRadiology, Department of Radiology and Imaging Sciences, University of Arizona, Tucson, AZ, USA

8 Neurological Surgery, Thomas Jefferson University, Philadelphia, PA, USA